Journal of Membrane Science 652 (2022) 120447

Contents lists available at ScienceDirect

Journal of Membrane Science

journal homepage: www.elsevier.com/locate/memsci

Contact angle screening and asymmetric dual-phase CO_2 separation membranes

Wen Xing [a,*], Anne Støre [b]

[a] SINTEF Industry, Thin Film and Membrane Technology, PO. Box 124, Blindern, NO, 0314, Oslo, Norway
[b] SINTEF Industry, Metal Production and Processing, P.O. Box 4760, Torgarden, NO, 7465, Trondheim, Norway

ARTICLE INFO

Keywords:
Wettability
CO_2 separation membrane
Oxides
Asymmetric membrane

ABSTRACT

Dual-phase CO_2 separation membrane consisting of molten carbonates confined in a solid matrix can separate CO_2 at high temperatures. The contact angle of molten carbonates to different oxides that can potentially serve as membrane supports was screened between 450 and 650 °C. These oxides have different electrical transport properties, including oxide ion, mixed, and electronic conducting. The contact angles vary between 80° and 10° for different materials. Asymmetric membranes were fabricated using wettable oxide ion conductors BTM and CGO ($Bi_{0.8}Tm_{0.2}O_{1.5}$ and $Ce_{0.8}Gd_{0.2}O_{2-\delta}$) infiltrated with molten carbonates supported by the most "non-wetting" oxide BPR ($Bi_{0.8}Pr_{0.2}O_{1.5}$) selected in the contact angle screening. The membranes show CO_2 flux in the range of 0.035–0.35 ml/min cm^2 at temperatures from 500 to 650 °C. Compared to a symmetric membrane with similar total membrane thickness, the asymmetric architecture significantly reduces the effective membrane thickness and increases CO_2 flux. After the CO_2 flux measurements, the membrane was examined with SEM and EDS mapping, showing that the molten carbonates were mainly confined within the top membrane and sealing area without penetrating the support layer.

1. Introduction

Molten carbonates infiltrated in a solid matrix can serve as a CO_2 separation membrane at temperatures above 500 °C. It is possible to integrate this dual-phase CO_2 separation membrane to processes directly at high temperatures, resulting in potential energy savings compared to the commercially available lower temperature polymeric membranes [1,2]. The transport properties of the membrane can be tailored by applying different solid matrices. The solid matrix provides compensating transport of charge carriers to the carbonate ions in the molten carbonates resulting in a net transport of gases. For instance, electronic conducting solid matrix leads to transport both O_2 and CO_2 simultaneously (oxygen needs to present in the feed side), and oxide ion conducting matrix leads to only CO_2 transport [3]. The flexible transport properties of these membranes have raised interest for application in several processes where separation of CO_2 or both CO_2 and O_2 is required. These encompass carbon capture and sequestration (CCS) applications for high temperature CO_2 separation in pre- and post-combustion CO_2 capture processes [4] and oxyfuel combustion, as well as in steam/dry reforming membrane reactors [5–8]. In addition, the gas selectivity towards CO_2 for the dual-phase membrane is infinite in theory providing the membrane an advantage for use in processes where high selectivity is needed [9].

Membranes have been reported using various solid matrix, e.g., metals [5,10], oxide ion conductors (Gd- and Sm-doped CeO_2 [11,12], stabilized zirconia [11,13,14] and $Bi_{1.5}Y_{0.3}Sm_{0.2}O_3$ [15,16]), mixed electron and oxide ion conductors ($La_{0.6}Sr_{0.4}Co_{0.8}Fe_{0.2}O_{3-\delta}$ [17,18]) and non-conductive ceramics such as alumina [11]. The asymmetric architecture of this type of membrane was firstly reported by using $Bi_{1.5}Y_{0.3}Sm_{0.2}O_3$ as "non-wetting" support and an oxide ion or mixed conductor as the matrix for holding molten carbonates. The method effectively reduces the membrane thickness and increases the CO_2 flux [8,13,14]. A schematic illustration of this asymmetric membrane is shown in Fig. 1 by considering only using the oxide ions conduction as the compensating charge carrier to the molten carbonate ions.

Due to the liquid nature of molten carbonates, one of the most critical aspects for symmetric membranes to work is to confine the molten carbonates in the membrane layer. Research on engineered hollow-fibers has shown that they can immobilize the carbonates and control their distribution [19]. Another approach is to use the "non-wetting" support to limit the percolation of the molten carbonates in an asymmetric membrane architecture. In previous reports, only BYS

* Corresponding author.
E-mail address: wen.xing@sintef.no (W. Xing).

https://doi.org/10.1016/j.memsci.2022.120447
Received 20 January 2022; Received in revised form 21 February 2022; Accepted 8 March 2022
Available online 10 March 2022

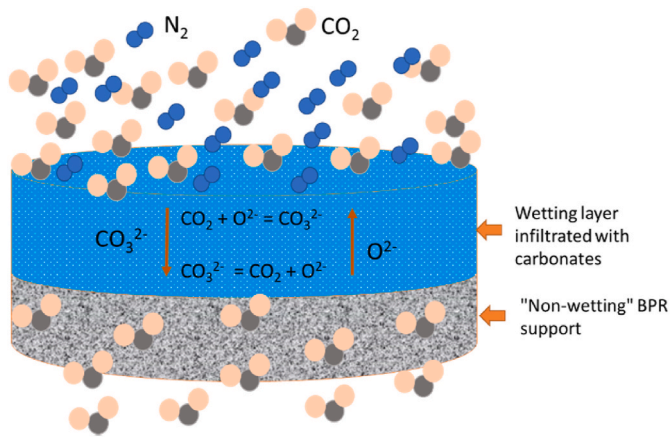

Fig. 1. CO_2 separation in an asymmetric dual-phase CO_2 separation membrane with "non-wetting" support. Oxide ions were chosen as the compensating charge carrier to the molten carbonate ions.

Table 1
Abbreviations of candidate materials for contact angle screening and classification of their electric properties.

Abbreviations	Compositions	Conduction types
LSM	$(La_{0.8}Sr_{0.2})_{0.99}MnO_3$	Electronic
PSF	$Pr_{0.8}Sr_{0.2}FeO_3$	Mixed
BVC	$Bi_2V_{0.9}Cu_{0.1}O_{5.5}$	Oxide ion
BPR	$Bi_{0.8}Pr_{0.2}O_{1.5}$	Oxide ion
BTM	$Bi_{0.8}Tm_{0.2}O_{1.5}$	Oxide ion
BYO	$Bi_{1.5}Y_{0.5}O_3$	Oxide ion
BYS	$Bi_{1.5}Y_{0.3}Sm_{0.2}O_3$	Oxide ion
BCO	$Bi_{20}Co_6O_{39}$	Oxide ion

($Bi_{1.5}Y_{0.3}Sm_{0.2}O_3$) was used, and the contact angle between molten carbonates and ceramics was seldom measured. The contact angle is defined as a measure of the ability of a liquid to wet the surface of a solid phase, and the value is determined by the angle between the liquid/solid interface and the tangent to the liquid/gas interface. Therefore, in this work, we focus on exploring "non-wetting" materials majorly based on doped Bi_2O_3 and measuring the contact angles for these materials at different temperatures. Bi_2O_3 has high oxide ion conductivity in its high temperature cubic phase (δ-phase), and the phase transition occurs at 700 °C. The low temperature phases (α-phase, β-phase, and γ-phase) show significantly lower oxide ion conductivity. However, the high temperature cubic phase can be stabilized down to room temperature by doping with rear-earth elements. Stabilized δ-Bi_2O_3 outperforms state-of-the-art oxide ion conductors such as doped ceria and zirconia. Among the lanthanide stabilized Bi_2O_3, thulium-doped (BTM) exhibited high phase stability at lower temperatures and high oxide ion conductivity due to its suitable ionic radius for attaining the cubic δ-Bi_2O_3 phase [20]. For archiving a higher CO_2 flux, BTM was used together with 20% gadolinium doped ceria (CGO) in the functional membrane layer in this work.

The materials investigated in this work include electronically conducting perovskite that is used for an electrode in SOFC [21] and Bi_2O_3 based materials [22,23] that are oxide ion conducting with a potentially low wetting angle to molten carbonates in the light for the previous work by B.Lu, &c. The materials selected for wettability screening in this work are listed in Table 1, with abbreviations used in the coming sections.

2. Experimental

BTM, BPR, BYO, BYS, and BVC powders were synthesized by the solid-state reaction method. Bi_2O_3 (Sigma Aldrich, 99.9%), Tm_2O_3 (Alfa Aesar, 99.9%), Pr_6O_{11} (Alfa Aesar, 99.9%), Y_2O_3 (Sigma Aldrich, 99.9%), V_2O_5 (Alfa Aesar, 99.6%), CuO (Alfa Aesar, 99.7%) and Sm_2O_3 (Sigma Aldrich, 99.9%) were used to produce ceramic powders. Stoichiometric amounts of bismuth oxides and dopant oxides were mixed in an agate mortar and calcinated at 750 °C for 10 h. LSM and PSF powers were produced by Cerpotech AS, Norway and CGO is produced by Marion Technologies, France. The powders were pressed into pellets in a 21 mm die with 3-ton loading. For the series of doped Bi_2O_3 oxides, the sintering temperature was 900 °C, and it was 1350 °C for LSM and PSF. BCO was sintered at the lowest temperature at 800 °C. The sintering time used for all the pellets is 6 h at each composition's sintering temperature, and the heating and cooling rates are 120 °C/h. The relative density for all the pellets is approximately 90%–95%, except for the BVC pellet, which is harder to sinter and has a relative density of about 85%. The phase purity for prepared samples was investigated using X-ray diffraction (PANalytical Empyrean) equipped with Cu Kα radiation at a scanning rate of 4° min^{-1} in 2θ range from 10° to 80°, and the microstructure of the BPR membrane support was characterized by a scanning electron microscope (Nova NanoSEM 650).

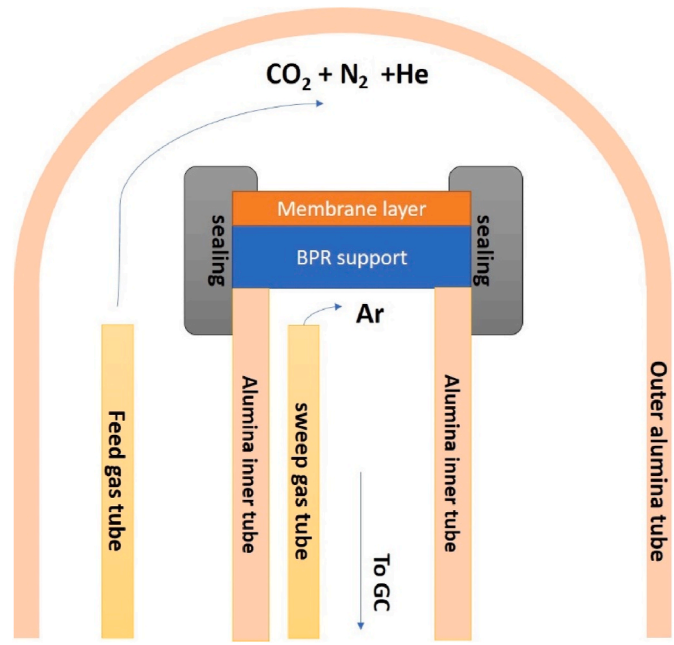

Fig. 2. Schematic illustration of the asymmetric membrane and the testing unit for the CO_2 flux measurements in a ProboStat™ measurement cell.

For the contact angle measurements, cylinders of the ternary eutectic carbonates mixture (32.1 wt% Li_2CO_3, 33.4 wt% Na_2CO_3, and 34.5 wt% K_2CO_3) with the dimension of 1 mm Ø × 2 mm were pressed. The cylinder was placed on the pellet and loaded in an optical dilatometer (Misura ODHT, Expert System Solutions, Italy). The furnace was heated from room temperature to 660 °C with a heating rate of 5 °C/min. A camera was taking pictures of the silhouette of the cylinder every 5 s. From these pictures, the wetting angle could be determined manually. The carbonate mixture melted around 400 °C, and the wetting angle was obtained every 10° between 450 and 650 °C. In this case, the angle between the molten carbonate/oxides interface and the tangent to the molten carbonate/air interface was measured.

For fabricating asymmetric membranes, the "non-wetting" power of BPR with 30 vol % food-grade starch powder and the membrane layer powder consisting of BTM and CGO (1:1 vol ratio) was co-pressed into green pellets followed by sintering at 900 °C for 6 h. The sintered pellet membranes were sealed to an alumina support tube using Aremco™ ceramic sealant and mounted in a ProboStat™ measurement cell (Nor-ECs, Norway). The sealing was achieved when the carbonates infiltrated into the membrane layer and the sealant at temperatures above the

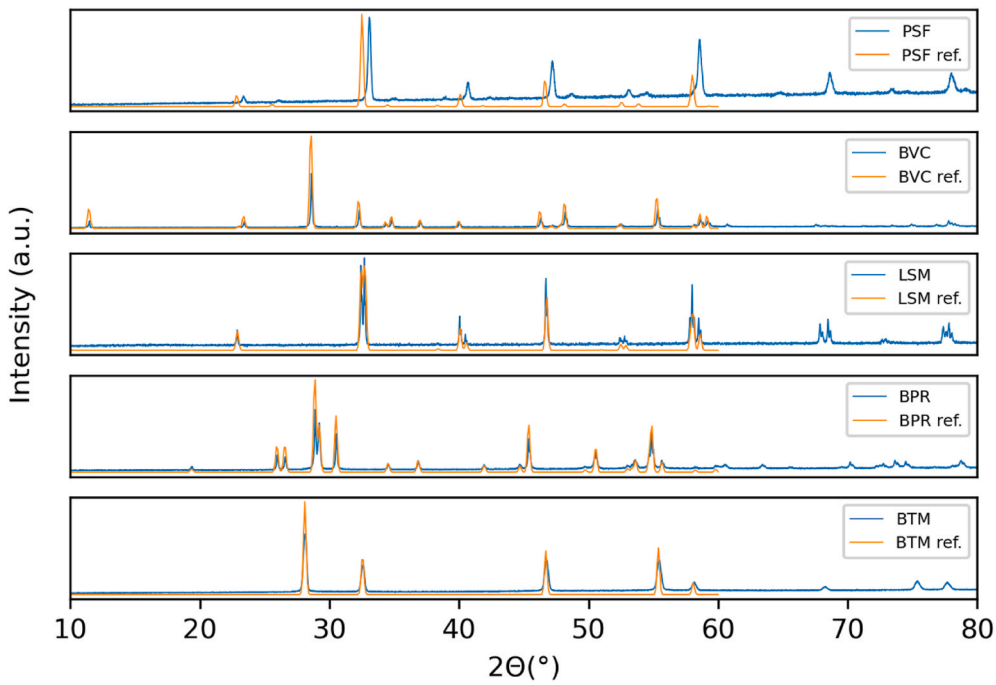

Fig. 3. XRD patterns were observed for different oxide pellets and compared with the reference peaks from the ICSD database.

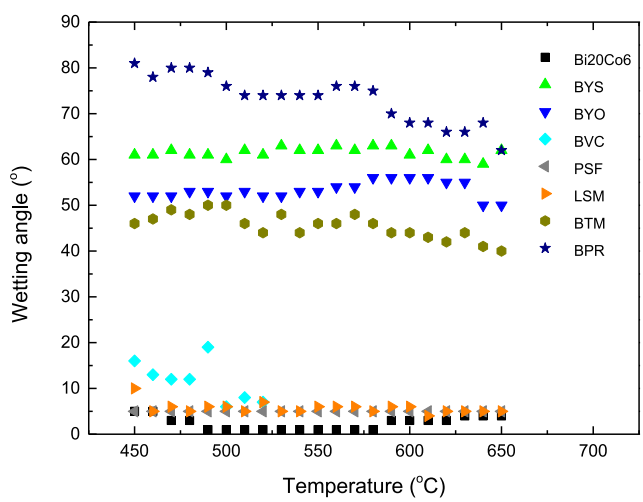

Fig. 4. The contact angle of the molten carbonates towards the solid support materials at temperatures from 450 to 650 °C.

melting point of carbonates. Mass flow controllers were utilized to supply CO_2, He and N_2 as feed gas mixtures, and Ar as sweep gas with a flow rate ranging from 1 to 100 ml/min. Permeation was measured with a Varian CP-4900 gas chromatograph (GC). An S-type thermocouple was placed close to the membrane, which was inserted into a vertical tubular furnace. The leakage was monitored by measuring the helium and nitrogen concentration in the sweep gas. During the experiments, the recorded helium concentration was in the range of a few to a few tens of ppm, and the N_2 concentration was in the range of tens of ppm. Both gases are on the detecting limit of the GC instrument used in the author's lab. The calculated helium and nitrogen leaking flux assuming a Knudsen-type diffusion at the lowest temperature with the lowest CO_2 flux is around 100 times lower than the CO_2 flux. Since the leakage is minor and the absolute values can deviate, the author did not record the leakage and shown in the plot but instead claimed a below 5% leakage rate for the most safety. A schematic illustration for the measurement cell with samples loaded is shown in Fig. 2.

3. Results and discussion

3.1. Materials characterizations and wettability

Synthesized oxides pellets were characterized by XRD, and the results are shown in Fig. 3 compared with the references data from Inorganic Crystal Structure Database (ICSD) database. The synthesized pellets correspond well with the reference data except for PSF, where the peaks are systematically shifted about 0.5° to the reference data, probably due to slight sample displacement. For BTM, the reference was 20% Er-doped Bi_2O_3 ($Bi_{0.8}Er_{0.2}O_{1.5}$) with a similar structure due to the database's lack of the BTM data.

Wetting angles of molten ternary eutectic molten carbonates towards the oxides under atmosphere conditions at temperatures between 450 °C and 650 °C are shown in Fig. 4. BPR shows the highest contact angle among all the tested oxides ranging between 80° and 60°. For BYS, BYO, and BTM, lower contact angles were observed, and the variation of contact angle at different temperatures is less significant than BPR. Molten carbonates can wet LSM and PSF, and Bi20Co6 with contact angles below 10°. Among all the candidate materials, significant reactivity between molten carbonates and BVC was observed. The contact angle observed of molten carbonates on these bismuth-based oxides is comparable to that observed on transition metals such as gold, copper, and nickel [24]. Since the contact angles measured in this work for all oxides are below 90°, by criteria of surface wetting (below 90°), the molten carbonates are wettable to all the samples. However, we used the term "non-wetting" for the high contact angle oxide of BPR, and this is for distinguishing it from these oxides having contact angles below 10°. In this work, the influence of surface roughness on carbonates' wettability was not considered. All the measurements were done on the surface of as-prepared pellets, which most likely can represent the surface for preparing the asymmetric membranes.

Pictures taken after the contact angle measurement when the samples were cooled down to room temperature are shown in the left part of Fig. 5. The molten carbonates are placed near the edge of the pellets due to the need for a good camera focusing. The pictures showing the molten

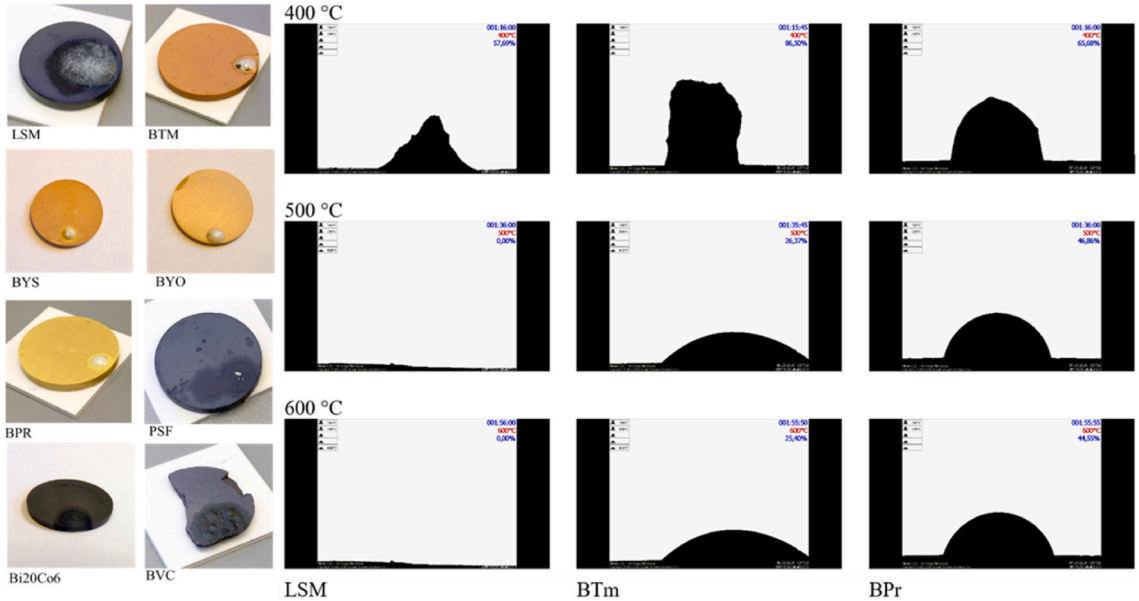

Fig. 5. Pictures to the left show the molten carbonates on the oxide pellets after the contact angle measurements. Example pictures taken during the contact measurements are shown in the right part.

carbonate on pellets in a furnace at different temperatures can be found in the right part of Fig. 5 for materials LSM, BTM and BPR.

3.2. CO_2 flux measurement

Three asymmetric membranes were fabricated by the same procedure with same composition in this work used for the flux measurement. As we can see from Fig. 6 (a), CO_2 fluxes for the three BPR-supported asymmetric membranes show similar behavior indicating a good reproducibility of the results, and the values range from 0.035 to 0.35 ml/cm^2 at temperatures between 550 and 650 °C. The thicknesses of the three asymmetric membranes are about1.2 mm with 0.2 mm for the membrane layer and 1.0 mm for BPR porous support. In the bottom part of Fig. 6, CO_2 flux for a symmetric membrane made from porous ceria (1.1 mm thick) with similar total thickness is included for comparison. About one order of magnitude higher CO_2 flux than the symmetric membrane was achieved for asymmetric membranes, primarily due to the significantly reduced effective membrane thickness. The measured CO_2 flux data for the asymmetric membrane is in line with the literature measured at an extended range of temperatures, as shown in Fig. 6 (b). The membrane layer thickness from the literature ranges from 0.1 to 0.15 mm, while our membrane layer has a thickness of 0.2 mm.

For dual-phase CO_2 separation membrane, both oxide ion and carbonate ion conduction play critical roles for CO_2 transport according to Eq. (1):

$$j_{CO_2} = j_{CO_3^{2-}} = \frac{RT}{2F^2L}\int_{sweep}^{feed} \sigma_{CO_3^{2-}} t_{O^{2-}}\, d\ln p_{CO_2} = \frac{RT}{2F^2L}\int_{sweep}^{feed} \frac{\sigma_{CO_3^{2-}}\sigma_{O^{2-}}}{\sigma_{CO_3^{2-}}+\sigma_{O^{2-}}}\, d\ln p_{CO_2} \quad (1)$$

where the CO_2 flux (j_{CO_2}) at a temperature (T) is described as a function of membrane thickness (L), oxide ion ($\sigma_{O^{2-}}$) and carbonate ion ($\sigma_{CO_3^{2-}}$) conduction, and the CO_2 partial pressure gradient from feed to sweep side. R and F in Eq. (1) are gas constant and Faraday constant, respectively. The equation is valid only if there are barely oxide ion and carbonate ion conductions involved and the term $\frac{\sigma_{CO_3^{2-}}\sigma_{O^{2-}}}{\sigma_{CO_3^{2-}}+\sigma_{O^{2-}}}$ usually called ambipolar conductivity [3].

From Eq. (1), a linear relationship between the CO_2 flux and the inverse of sample thickness applies for a membrane under defined CO_2 partial pressure gradient and temperature. Therefore, considering the effective thickness difference between symmetric and asymmetric membranes in Fig. 6, the asymmetric membrane should be about 5.5 times higher than the CGO symmetric membrane under the same measurement conditions. However, the observations were about 10 times higher. The enhanced performance besides the thickness effect for the asymmetric membrane could be due to the higher oxide ion conductivity of BTM employed in the asymmetric membrane than doped ceria. In principle, if we could use BTM alone as the membrane support, we probably could achieve higher CO_2 flux due to the higher oxide ion conductivity for BTM. However, molten carbonates do not highly wet the surface of BTM with about 45° contact angle measured as shown in the section above. So, 50 volumetric CGO was used together with BTM to improve the wettability.

The ambipolar conductivity term in Eq. (1) is determined generally by the two conductivities whichever is lower and, in this case, the oxide ion conduction. The calculated activation energy for the CO_2 flux of the asymmetric membrane is approximately 108 kJ/mol in the measurement temperature range, which is in between the oxide ion conductivity activation energy for doped CeO_2 (86 kJ/mol) [25] and Tm doped Bi_2O_3(106–125 kJ/mol) at lower temperatures [20]. Compared to the low activation energy for carbonate ion conductivity in the melt, the high activation energy indicated the CO_2 flux is limited by the oxide ion conductivity in the membrane layer.

In this work, the absolute pressure applied to both the feed and sweep side of the membrane is ambient. The absolute pressure difference across the membrane might be applied in practical applications. Therefore, knowing the absolute pressure tolerance is critical for this membrane type. Depending on the pore size and wettability of carbonates towards the membrane matrix, the pressure tolerance of this type of membrane was calculated in Ref. [9]. Recent work shows by experiment that this type of dual-phase CO_2 separation membrane can tolerate 14 bar absolute pressure difference for a tubular architecture with a small pore size [26].

After the measurements, one asymmetric membrane was dismounted from the measurement cell checked by SEM. One piece of the membrane is shown in Fig. 7 (a) and compared with a pen in (b). The SEM picture of

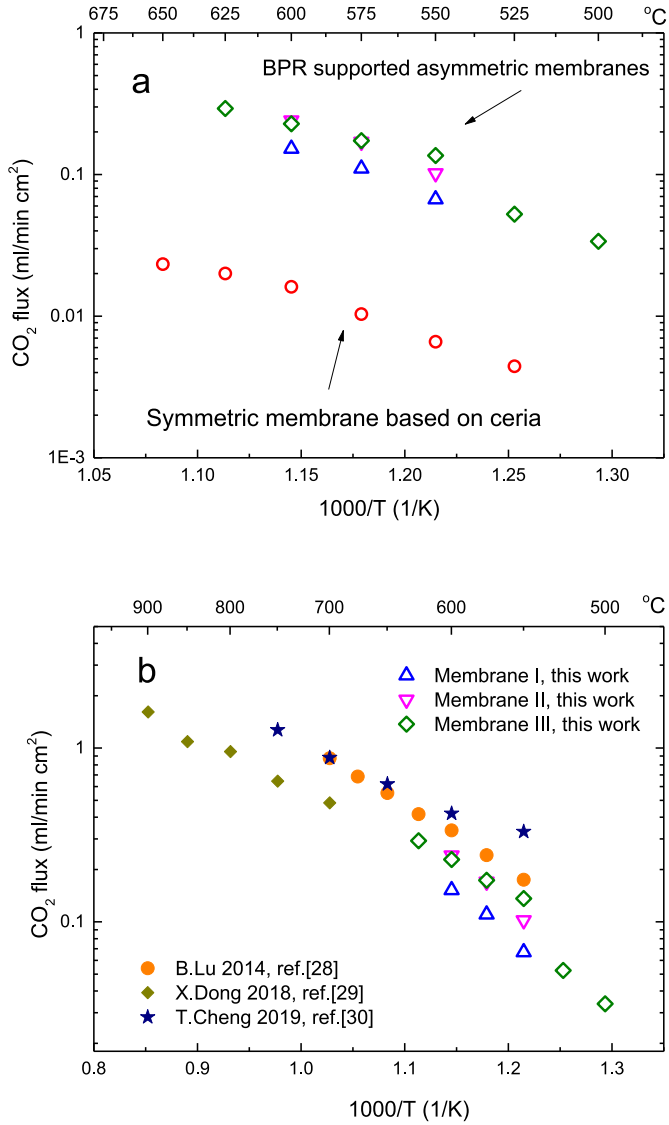

Fig. 6. (a) CO_2 flux of the asymmetric membranes at different temperatures. The CO_2 flux for a symmetric ceria-based membrane with a similar thickness (1.1 mm) is included for comparison [27]. The results for three similar samples of asymmetric membranes are shown in different colors at the top. (b) Comparison of the asymmetric membrane CO_2 flux in this work to the literature data of asymmetric membrane with similar membrane thickness and doped CeO_2 as membrane support layer [28–30]. (For interpretation of the references to color in this figure legend, the reader is referred to the Web version of this article.)

the membrane and sealant on the edge is shown in (c). EDS mapping (d) shows that the membrane layer and sealant area are enriched with Na or K, which differs from the BPR support. The carbonates melt was confined within the membrane layer, and the sealing area and the "non-wetting" BPR support have little carbonate infiltration detected, showing the asymmetric architecture's nature.

The asymmetric membrane consists of three materials with different thermal expansion coefficients (TECs) and sintering properties. CGO has the TEC of 12.2×10^{-6} K^{-1} and sinters at temperature above 1400 °C [31]. BPR has the TEC of 13×10^{-6} K^{-1} and sinters at about 900 °C [32]. BTM, however can have TEC like δ-Bi_2O_3 of more than 20×10^{-6} K^{-1} and sinters at similar temperature to BPR [33]. Despite these different properties of the compositions, the co-pressed membranes are sintered without creaks but slightly convex were observed. This slightly convex shape drives the molten carbonates move to the side and causing leakages after about 2 days at 650 °C. However, due to the low vapor pressure of molten carbonates, we believe that better engineering of the asymmetric membrane e.g., making membrane flatter, or smaller pore size to increase capillary force to confine the molten phase in the pores can well extend the lifetime of the asymmetric membrane. Dual-phase membrane and molten carbonate fuel cells has demonstrated months and years stable operation, relying on the same principals.

4. Conclusion

Eight candidate oxides with different electric transport properties were screened for their contact angle towards the ternary eutectic molten carbonates at temperatures between 450 and 650 °C. The contact angles were obtained between 80° to below 10°. Asymmetric membranes were successfully made by using the most "non-wetting" BPR oxide as support together with ceria and BTM as membrane layer. The CO_2 flux achieved with the asymmetric membranes is in the range of 0.035–0.35 ml/min $cm^{2,}$ which is about one order of magnitude higher than for symmetric membranes with similar membrane thickness. SEM and EDS mapping results reveal the expected distributions of the molten carbonates in the membrane where the molten carbonates were confined in the membrane layer and sealant but not in the BPR support layer. The new "non-wetting" materials found in this work can potentially be used to make high-performance supported dual-phase CO_2 separation membranes.

Author statement

Wen Xing: Conceptualization, Methodology, Project administration, Writing - Original Draft, Funding acquisition.**Anne Støre:** Investigation, Methodology, Writing - Review & Editing.

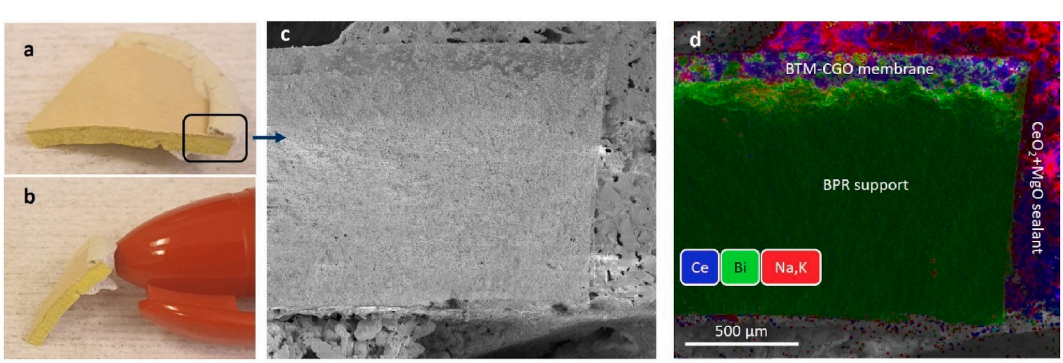

Fig. 7. (a) and (b) membrane after CO_2 flux measurement and its relative size to the cap of a pen, respectively, (c) the microstructure of the membrane after flux testing, (d) EDX mapping of the corresponding area of picture (c) concerning elements of Ce, Bi, and alkaline elements in the carbonates.

Declaration of competing interest

The authors declare that they have no known competing financial interests or personal relationships that could have appeared to influence the work reported in this paper.

Acknowledgments

MOCO3 project was granted through the M-ERA.NET program, and major financial support from the Research Council of Norway (RCN) for MOCO3 project (272688) is gratefully acknowledged to this work. MOLCAR project (NOR/POLNORCCS/MOLCAR/00-17/2020-00) supported by The National Center for Research and Development (NCBR), Poland is also acknowledged for financial support to finish this paper.

References

[1] T. Chen, Z. Wang, J. Hu, M.H. Wai, S. Kawi, Y.S. Lin, High CO_2 permeability of ceramic-carbonate dual-phase hollow fiber membrane at medium-high temperature, J. Membr. Sci. 597 (2020) 117770.
[2] Y.S. Lin, Inorganic membranes for process intensification: challenges and perspective, Ind. Eng. Chem. Res. 58 (2019) 5787–5796.
[3] W. Xing, T. Peters, M.-L. Fontaine, A. Evans, P.P. Henriksen, T. Norby, R. Bredesen, Steam-promoted CO_2 flux in dual-phase CO_2 separation membranes, J. Membr. Sci. 482 (2015) 115–119.
[4] R. Anantharaman, T. Peters, W. Xing, M.-L. Fontaine, R. Bredesen, Dual phase high-temperature membranes for CO_2 separation - performance assessment in post- and pre-combustion processes, Faraday Discuss 192 (2016) 251–269.
[5] S.J. Chung, J.H. Park, D. Li, J.I. Ida, I. Kumakiri, J.Y.S. Lin, Dual-phase Metal−Carbonate membrane for high-temperature carbon dioxide separation, Ind. Eng. Chem. Res. 44 (2005) 7999–8006.
[6] M. Anderson, Y.S. Lin, Carbon dioxide separation and dry reforming of methane for synthesis of syngas by a dual-phase membrane reactor, AIChE J. 59 (2013) 2207–2218.
[7] T. Chen, Z. Wang, L. Liu, S. Pati, M.H. Wai, S. Kawi, Coupling CO_2 separation with catalytic reverse water-gas shift reaction via ceramic-carbonate dual-phase membrane reactor, Chem. Eng. J. 379 (2020) 122182.
[8] H.-C. Wu, Z. Rui, J.Y.S. Lin, Hydrogen production with carbon dioxide capture by dual-phase ceramic-carbonate membrane reactor via steam reforming of methane, J. Membr. Sci. 598 (2020) 117780.
[9] G.A. Mutch, L. Qu, G. Triantafyllou, W. Xing, M.-L. Fontaine, I.S. Metcalfe, Supported molten-salt membranes for carbon dioxide permeation, J. Mater. Chem. 7 (2019) 12951–12973.
[10] J. Fang, J. Tong, K. Huang, A superior mixed electron and carbonate-ion conducting metal-carbonate composite membrane for advanced flue-gas carbon capture, J. Membr. Sci. 505 (2016) 225–230.
[11] J.L. Wade, C. Lee, A.C. West, K.S. Lackner, Composite electrolyte membranes for high temperature CO_2 separation, J. Membr. Sci. 369 (2011) 20–29.
[12] M.L. Fontaine, T.A. Peters, M.T.P. McCann, I. Kumakiri, R. Bredesen, CO_2 removal at high temperature from multi-component gas stream using porous ceramic membranes infiltrated with molten carbonates, Energy Proc. 37 (2013) 941–951.
[13] B. Lu, Y.S. Lin, Synthesis and characterization of thin ceramic-carbonate dual-phase membranes for carbon dioxide separation, J. Membr. Sci. 444 (2013) 402–411.
[14] S. Sun, Y. Wen, K. Huang, A new ceramic–carbonate dual-phase membrane for high-flux CO_2 capture, ACS Sustain. Chem. Eng. 9 (2021) 5454–5460.
[15] Z. Rui, M. Anderson, Y. Li, Y.S. Lin, Ionic conducting ceramic and carbonate dual phase membranes for carbon dioxide separation, J. Membr. Sci. 417 (2012) 174–182.
[16] Y. Li, Z. Rui, C. Xia, M. Anderson, Y.S. Lin, Performance of ionic-conducting ceramic/carbonate composite material as solid oxide fuel cell electrolyte and CO_2 permeation membrane, Catal. Today 148 (2009) 303–309.
[17] M. Anderson, Y.S. Lin, Carbonate–ceramic dual-phase membrane for carbon dioxide separation, J. Membr. Sci. 357 (2010) 122–129.
[18] S. Zhuang, Y. Li, M. Zuo, X. Tan, B. Meng, N. Yang, S. Liu, Dense composite electrolyte hollow fibre membranes for high temperature CO_2 separation, Separ. Purif. Technol. 132 (2014) 712–718.
[19] M. Kazakli, G.A. Mutch, G. Triantafyllou, A.G. Gil, T. Li, B. Wang, J.J. Bailey, D.J. L. Brett, P.R. Shearing, K. Li, I. Metcalfe, Controlling molten carbonate distribution in dual-phase molten salt-ceramic membranes to increase carbon dioxide permeation rates, J. Membr. Sci. 617 (2021) 118640.
[20] A. Dapčević, D. Poleti, J. Rogan, A. Radojković, M. Radović, G. Branković, A new electrolyte based on Tm^{3+}-doped δ-Bi_2O_3-type phase with enhanced conductivity, Solid State Ionics 280 (2015) 18–23.
[21] J. Piao, K. Sun, N. Zhang, X. Chen, S. Xu, D. Zhou, Preparation and characterization of $Pr_{1-x}Sr_xFeO_3$ cathode material for intermediate temperature solid oxide fuel cells, J. Power Sources 172 (2007) 633–640.
[22] A.M. Azad, S. Larose, S.A. Akbar, Bismuth oxide-based solid electrolytes for fuel cells, J. Mater. Sci. 29 (1994) 4135–4151.
[23] A. Ramanan, J. Gopalakrishnan, C.N.R. Rao, Ternary bismuth oxides $Bi_{26-x}M_xO_{40-y}$ (M = Mg, Al, Co and Ni) related to α - Bi_2O_3, Mater. Res. Bull. 16 (1981) 169–174.
[24] J.M. Fisher, P.S. Bennett, Corrosion and wetting behaviour of metals and steels with molten alkali carbonates, J. Mater. Sci. 26 (1991) 749–755.
[25] A. Arabacı, M.F. Öksüzömer, Preparation and characterization of 10mol% Gd doped CeO_2 (GDC) electrolyte for SOFC applications, Ceram. Int. 38 (2012) 6509–6515.
[26] O. Ovalle-Encinia, J.Y.S. Lin, High-pressure CO_2 permeation properties and stability of ceramic-carbonate dual-phase membranes, J. Membr. Sci. 646 (2022) 120249.
[27] W. Xing, Z. Li, T. Peters, M.-L. Fontaine, M. McCann, A. Evans, T. Norby, R. Bredesen, Improved CO_2 flux by dissolution of oxide ions into the molten carbonate phase of dual-phase CO_2 separation membranes, Separ. Purif. Technol. 212 (2019) 723–727.
[28] B. Lu, Y.S. Lin, Asymmetric thin samarium doped cerium oxide–carbonate dual-phase membrane for carbon dioxide separation, Ind. Eng. Chem. Res. 53 (2014) 13459–13466.
[29] X. Dong, H.-C. Wu, Y.S. Lin, CO_2 permeation through asymmetric thin tubular ceramic-carbonate dual-phase membranes, J. Membr. Sci. 564 (2018) 73–81.
[30] T. Chen, Z. Wang, S. Das, L. Liu, Y. Li, S. Kawi, Y.S. Lin, A novel study of sulfur-resistance for CO_2 separation through asymmetric ceramic-carbonate dual-phase membrane at high temperature, J. Membr. Sci. 581 (2019) 72–81.
[31] P. Gao, A. Bolon, M. Taneja, Z. Xie, N. Orlovskaya, M. Radovic, Thermal expansion and elastic moduli of electrolyte materials for high and intermediate temperature solid oxide fuel cell, Solid State Ionics 300 (2017) 1–9.
[32] C. Ftikos, B.C.H. Steele, Electrical conductivity and thermal expansion of Bi_2O_3 doped with Pr, J. Eur. Ceram. Soc. 14 (1994) 501–504.
[33] P. Shuk, H.D. Wiemhöfer, U. Guth, W. Göpel, M. Greenblatt, Oxide ion conducting solid electrolytes based on Bi_2O_3, Solid State Ionics 89 (1996) 179–196.